

RADIAL TRANSMISSION LINE ANALYSIS OF MULTI-LAYER CIRCULAR STRUCTURES*

H. Hahn[†] and L. Hammons, C-AD, BNL, Upton, NY 11973, U.S.A.

Abstract

The analysis of multi-layer beam tubes is a frequent problem and is usually solved with axially propagating waves. This treatment is ill suited to a short multi-layer structure such as the present example of a ferrite covered ceramic break in the beam tube at the ERL photo-cathode electron gun. This paper demonstrates that such structures can better be treated by radial wave propagation. The theoretical method is presented and numerical results are compared with measured network analyser data and Microwave Studio generated simulations. The results confirm the concept of radial transmission lines as a valid analytical method.

INTRODUCTION

An Energy Recovery Linac (ERL) is being constructed at this laboratory for the purpose of research towards an envisioned Electron Ion Collider. One of the pertinent topics is damping of Higher Order Modes (HOM). In this ERL, the damping is provided by ferrite absorbers in the beam tube. A modified version thereof, a ceramic break surrounded by ferrite, is planned for the superconducting electron gun. The damper here is located at room temperature just outside of the gun. If used in a cavity chain, the ceramic break is in the vacuum tube at helium temperature whereas the ferrite is moved into the cryostat insulating vacuum allowing higher temperatures. The general properties of the ferrite HOM dampers have been published [2] but are more detailed in this paper.

The “ferrite break”, shown in Fig. 1, can be simplified for the analysis into a structure with a radial sequence of circular symmetric layers. The electromagnetic properties of multi-layer beam tubes have usually been treated by many authors, with the axial transmission line solution [3]. The short axial length and the presence of the metallic boundary disks points to the treatment as “radial” transmission line, with its basic concept discussed in Section 2. For the purpose of this study, a simple model with a glass tube replacing ceramic but equal in length to the ferrite disks was conceived. The impact of glass on the ferrite model was numerically analyzed in the Wolfram Mathematica program. Section 3 treats the break impedance via the network analyzer measurements of the transmission coefficients, primarily S21, that were performed on the model with a central conductor (rod).

* Work supported by B.S.A, LLC under Contract No. DE-AC02-98 CH10886 with the U.S. DOE.

[†] hahn@bnl.gov

The measured data are also compared with simulation results from the CST Microwave Studio. For Section 4, the central rod was removed and the additional measurements and simulations confirmed the break damping properties, although they vary with frequency.

RADIAL TRANSMISSION LINE

Radial propagation in a “wave guide horn”, formed by two perfectly conducting annular disks, spaced with a gap, g can be described in formalism similar to the better-known axial propagation in straight tubular wave guides [4, 5]. Assuming harmonic time dependence, e^{jkt} , and circular coordinate system, r, φ, z , the radial field propagation is fully defined by the transverse components $E_\varphi, E_z, H_\varphi, H_z$ in analogy to the $E_r, E_\varphi, H_r, H_\varphi$ for axial propagation. This geometry allows transverse magnetic TM and electric TE modes. In a material with normalized ϵ and μ , the radially propagating fields are derived in terms of Hankel functions from the potential,

$$\begin{cases} u^{TM} \\ u^{TE} \end{cases} = \begin{cases} \cos k_{zn} \\ \sin k_{zn} \end{cases} \cos(m\varphi) \begin{cases} H_m^{(1)}(v_n r) \\ H_m^{(2)}(v_n r) \end{cases}, \begin{cases} n = 0, 1, 2, \dots \\ n = 1, 2, 3, \dots \end{cases},$$

where $k = \omega / c$, $k_{zn} = n\pi / g$ and $v_n = \sqrt{\epsilon\mu k^2 - k_{zn}^2}$.

Considering here only TM_{mpn} modes yields the fields

$$E_z = \begin{cases} H_m^{(1)}(v_n r) \\ H_m^{(2)}(v_n r) \end{cases}, H_\varphi = -j \frac{\epsilon k}{v_n} \begin{cases} H_m^{(1)'}(v_n r) \\ H_m^{(2)'}(v_n r) \end{cases}$$

and the radial wave impedance of an out-going wave

$$Z_{rn} = -\frac{E_{zn}}{H_{\varphi n}} = j \frac{v_n}{k\epsilon} \frac{H_0^{(2)}(v_n r)}{H_1^{(2)}(v_n r)} \rightarrow j \frac{H_0^{(2)}(kr)}{H_1^{(2)}(kr)} \text{ in vacuo.}$$

The analysis of the ferrite break with its ceramic and ferrite layer is done in analogy to Hahn’s axial matrix method treatment of multi-layer beam tubes [6]. The radial transmission matrix for a single mode from the outer radius to a radius within the layer is:

$$\begin{pmatrix} E_{zn}(r) \\ H_{\varphi n}(r) \end{pmatrix} = M_n(r, r_o) = \begin{bmatrix} m_{nee}(r, r_o) & m_{neh}(r, r_o) \\ m_{nhe}(r, r_o) & m_{nhh}(r, r_o) \end{bmatrix} \begin{pmatrix} E_{zn}(r_o) \\ H_{\varphi n}(r_o) \end{pmatrix}$$



Figure 1: Ceramic break with ferrite HOM damper.

The elements of the field transfer matrix are found

$$m_{nee}(r, r_o) = j \frac{\pi}{4} v_n r_o \left[H_0^{(2)}(v_n r) H_1^{(1)}(v_n r_o) - H_0^{(1)}(v_n r) H_1^{(2)}(v_n r_o) \right]$$

$$m_{neh}(r, r_o) = -\frac{\pi}{4} \frac{v_n^2 r_o}{\epsilon k} \left[H_0^{(2)}(v_n r) H_0^{(1)}(v_n r_o) - H_0^{(1)}(v_n r) H_0^{(2)}(v_n r_o) \right]$$

$$m_{nhe}(r, r_o) = -\frac{\pi}{4} \epsilon k r_o \left[H_1^{(2)}(v_n r) H_1^{(1)}(v_n r_o) - H_1^{(1)}(v_n r) H_1^{(2)}(v_n r_o) \right]$$

$$m_{nhh}(r, r_o) = -j \frac{\pi}{4} v_n r_o \left[H_1^{(2)}(v_n r) H_0^{(1)}(v_n r_o) - H_0^{(1)}(v_n r) H_1^{(2)}(v_n r_o) \right]$$

The field at the inner radius of a layer must be summed over the individual modes,

$$\begin{pmatrix} E_z(r_i) \\ H_\varphi(r_i) \end{pmatrix} = \begin{pmatrix} \sum_n E_{zn}(r_i) \\ \sum_n H_{\varphi n}(r_i) \end{pmatrix} = \sum_n M_n(r_i, r_o) \begin{pmatrix} E_{zn}(r_o) \\ H_{\varphi n}(r_o) \end{pmatrix}$$

In the case of several layers, the modes propagate uncoupled through the layers and the overall matrix is obtained by matrix multiplication of the individual matrices [6]. In contrast to the radial wave impedance of the infinitely extended layer given above, the impedance of a multi-layer finite structure is

$$Z_r = \frac{M_{ee}(r, r_o) Z(r_o) - M_{eh}(r, r_o)}{M_{hh}(r, r_o) - M_{he}(r, r_o) Z(r_o)}$$

which is reduced by a perfectly conducting outer tube to

$$Z(r_c) = -M_{eh}(r_c, r_o) / M_{hh}(r_c, r_o)$$

As a numerical test, the surface impedances of a ferrite ring with $\epsilon = 13$, $\mu = 29/(1+j2.5 f_{MHz})$ and an inner radius of $r_i = 75.4$ mm are shown in Fig. 2 for unbound, 4.9 mm thick with perfect conducting, or vacuum outside.

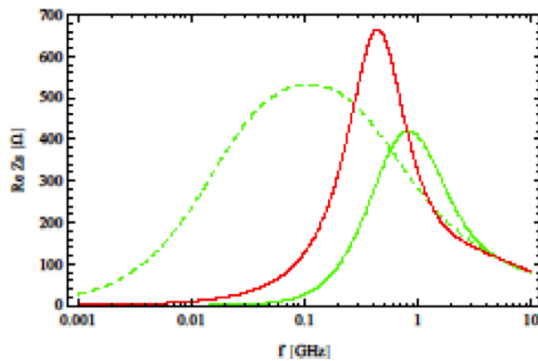


Figure 2: Impedance of a ferrite ring for unbound (dashed), vacuum (red) and shorted (green) outside .

IMPEDANCE OF THE BREAK

The intended gun cavity damping properties and the unintended beam coupling impedance are determined by the wall impedance at the inner layer of the break. The break can be represented by lumped impedance, different for each azimuthal field configuration, that together with the local H determines gun cavity damping or beam coupling impedance.

The complex geometry of the break effectively prevents the use of standard analytical methods to find its electromagnetic properties. Creating a simplified model transforms the break into a prototypical example for the radial transmission method. Computational results shown

in Fig. 3 follow directly from the radial transmission line treatment. Note that large Z values imply strong damping. One purpose of the present study was to establish the interaction of the relatively lossless ceramic (here glass) with the strong damping properties of the ferrite. The numerical results here point to a frequency dependent $Z(r_c)$, yet sufficient in the operational range.

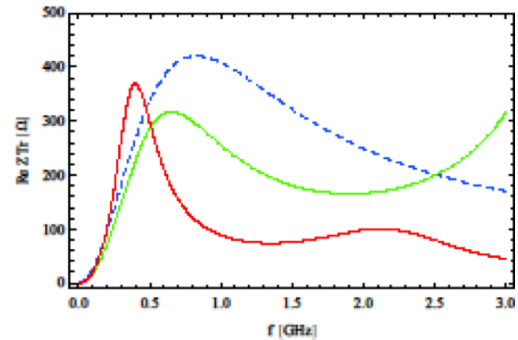


Figure 3: Break impedance of the model with ferrite and glass (red), with ferrite (green) and the wave impedance at the ferrite i. d. (dashed blue).

The computer model shown in Fig. 4 leads to the comparisons of analytical with MWS simulations. In addition, a physical model was produced for S_{21} measurements with a network analyzer. This model was assembled from the ferrite plates intended for the gun damper, but with the ceramic break replaced by a glass tube. The cavity model is flexible and can be assembled in several configurations allowing to study it as reference cavity without ferrite or glass, as pure ferrite damper, as pill box with glass ring, or in its final form as glass break with ferrite layer.

The break impedance is now obtained either from the S_{21} measurements as pictured in the setup in Fig. 5 or the frequency domain simulations with the MWS model. Both measurements and simulations involve N type EIA couplers with unknown frequency dependence and transformer ratios that limit a direct comparison of the results in Fig 6 to the analytical results in Fig. 3. Note also that S_{21} and Z_{Tr} have inverse impact.

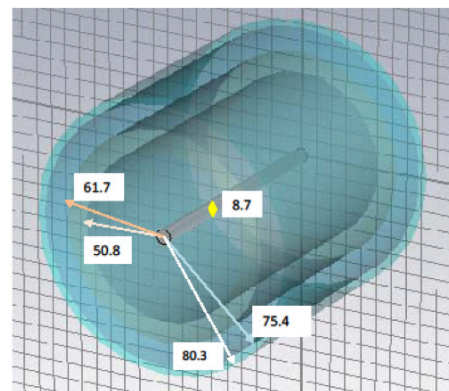


Figure 4: Break model for MWS simulations and radial transmission analysis.

Considering Fig. 6, one sees the glass induced changes of the achievable ferrite damping to be dependent on frequency. The oscillations with frequency are believed to be caused by the intrinsic cavity resonances in axial direction that are made possible by the insertion of the central conductor marked as rod.

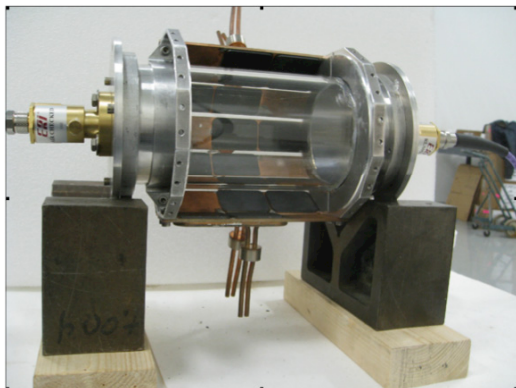


Figure 5: Setup for network analyzer measurements.

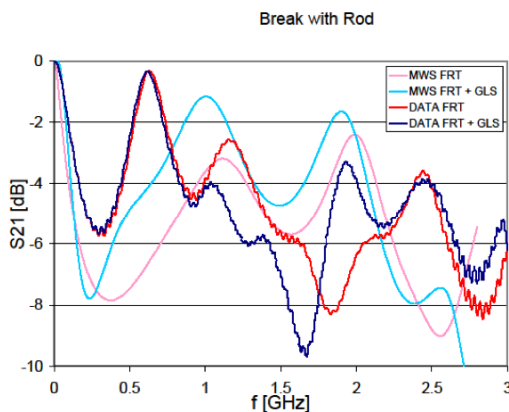


Figure 6: Forward scattering coefficient across the cavity.

Both, the damping of the gun cavity resonances and the coupling impedance seen by the beam generated by the break are best defined by its equivalent series impedance Z_{TR} . This impedance is conveniently measured as ratio of the S_{21} of the “device under test” divided by the S_{21} of the reference structure. In the present structure, the reference is provided by the damper structure without ferrite or the glass tube. The equivalent impedance follows then directly from the network analyzer measurement by using the conversion of the S_{21} data into forward impedance while applying an 810 nsec delay to represent the reference. Fig 7 shows the signal for the reference (gold) after the 810 nsec adjustment to avoid a negative real part of the impedance. Also shown here is the real part of the damper impedance, raw (light blue) and then with the delay applied (blue). The signal for the ferrite without glass is also given (red). The difference in strength here versus Fig. 3 is due to the unknown coupler transformer. It must be mentioned that this geometry provides only the impedance of TM modes with axial

electric fields since transverse electric modes are not excited by the axial conductor.

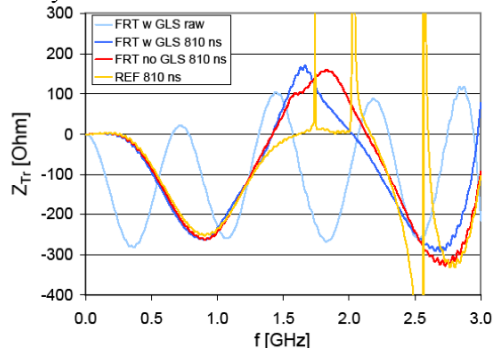


Figure 7: Series impedance of the break from S_{21} conversion.

DAMPING OF BREAK RESONANCES

In the cavity without central conductor, the lowest intrinsic TM_{01n} resonances are at ~ 1.39 and 1.71 GHz, but are strongly damped and frequency shifted resulting in the smeared-out S_{21} transmission curve in Fig. 8. The intrinsic and the damped resonances are found in the radial transmission theory by matching the break impedance, real and imaginary part, to the radial wave impedance at the inner ceramic radius, $jJ_0(kr_c) / J_1(kr_c) = Z_r$. The Q -value is found via $Q \approx k_{Re} / 2k_{Im}$ by “pulling” the lossless result, yielding $Q \leq 1$ for the TM_{010} mode at 466 MHz versus $Q_{MWS} \approx 0.97$.

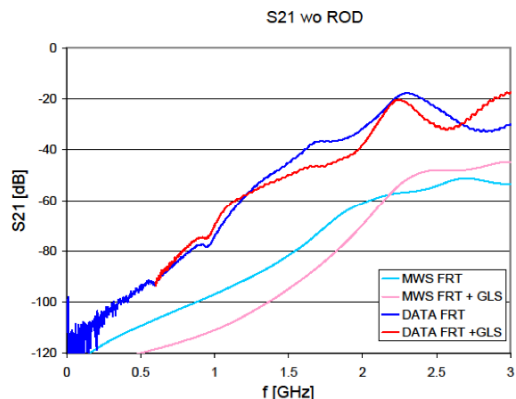


Figure 8: Achieved S_{21} signal damping, measured and simulated for ferrite alone and with a glass tube added.

REFERENCES

- [1] L. Hammons and H. Hahn., this conference.
- [2] H. Hahn et al., Phys. Rev. ST-AB, **13**, 121002 (2010)
- [3] B. W. Zotter and S. A. Kheifets, *Impedances and Wakes in High-Energy Particle Accelerators*, (World Scientific, Singapore, 1998)
- [4] N. Marcuvitz, in C. G. Montgomery, *Principles of Microwave Circuits* (McGraw-Hill Book Company, NY, 1948) p. 240.
- [5] H.-G. Unger, *Elektromagnetische Wellen I*, (F. Vieweg & Sohn, Braunschweig, 1967), p. 168.
- [6] H. Hahn, Phys. Rev. ST-AB, **13**, 012002 (2010)